Molecular Diversity (2020) 24:603–615
https://doi.org/10.1007/s11030-019-09967-y

ORIGINAL ARTICLE

Design, synthesis, antifungal activity, and structure–activity relationship studies of chalcones and hybrid dihydrochromane–chalcones

Marco Mellado[1] · Luis Espinoza[2] · Alejandro Madrid[3] · Jaime Mella[4] · Eduardo Chávez-Weisser[5] · Katy Diaz[2] · Mauricio Cuellar[6]

Received: 29 March 2019 / Accepted: 25 May 2019 / Published online: 3 June 2019

Abstract

A series of ten chalcones (**7a–j**) and five new dihydrochromane–chalcone hybrids (**7k–o**) were synthesized and identified using spectroscopic techniques (IR, NMR, and MS). All compounds were evaluated in vitro against the *B. cinerea* and *M. fructicola* phytopathogens that affect a wide range of crops of commercial interest. All compounds were tested against both phytopathogens using the mycelial growth inhibition test, and it was found that two and five compounds had similar activity to that of the positive control for *B. cinerea* (**7a** = 43.9, **7c** = 45.5, and Captan® = 24.8 µg/mL) and *M. fructicola* (**7a** = 48.5, **7d** = 78.2, **7e** = 56.1, **7f** = 51.8, **7n** = 63.2, and Mystic® = 21.6 µg/mL), respectively. To understand the key chalcone structural features for the antifungal activity on *B. cinerea* and *M. fructicola*, we developed structure–activity models with good statistical values (r^2 and q^2 higher than 0.8). For *B. cinerea*, the hydrogen bonding donor and acceptor and the atomic charge on C_5 modulate the mycelial growth inhibition activity. In contrast, dipole moment and atomic charge on $C_{1'}$ and the carbonyl carbon modify the inhibition activity for *M. fructicola*. These results allow the design of other compounds with activities superior to those of the compounds obtained in this study.

Graphic Abstract

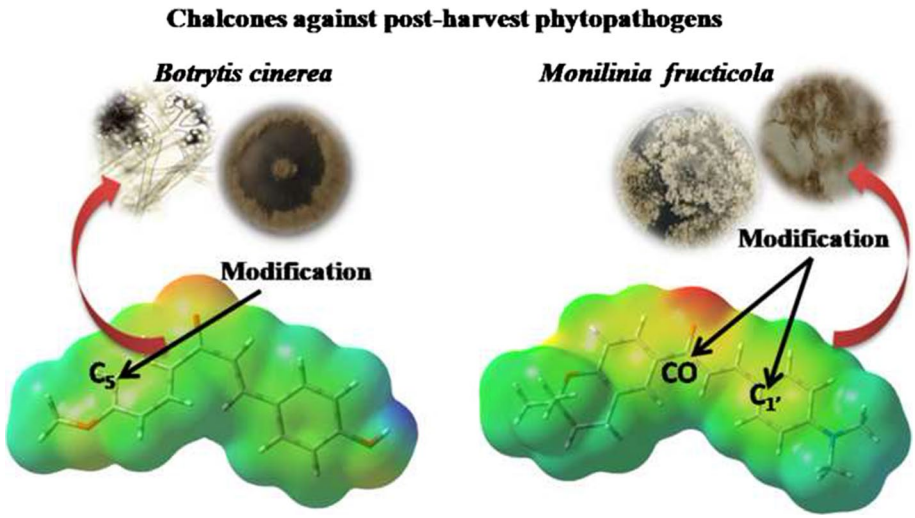

Electronic supplementary material The online version of this article (https://doi.org/10.1007/s11030-019-09967-y) contains supplementary material, which is available to authorized users.

Extended author information available on the last page of the article

Keywords *Botrytis cinerea* · *Monilinia fructicola* · Fungicides · Chalcones · Dihydrochromane · 2D-QSAR

Introduction

Botrytis cinerea and *Monilinia fructicola* (Winter) Honey are superior phytopathogenic fungi of the ascomycete family. They are responsible for "gray mold" and "brown rot" diseases that attack a wide variety of fruits, vegetables, and field crops around the world (e.g., grapes), causing significant economic losses in the pre- and postharvest stage in the crops [1–4]. In fact, fungus control is very important in grape-producing countries such as Chile, France, Germany, Italy, South Africa, and the USA, as well as in the wine-producing and exporting countries [5].

In this context, over the past decades, chemical fungicides have been used in pre- and postharvest periods to prevent and control the diseases caused by both of these pathogens. However, the fungi have developed resistance to some conventional fungicides, particularly benzimidazoles and dicarboximides [6]. In fact, these compounds cause severe damage to the environment, human beings, and beneficial microbiota in agriculture and should be replaced with less toxic compounds [7].

Due to the mentioned above, phenolic compounds emerge as a potential source of control of phytopathogen [8–12]. For example, chalcones are natural compounds that belong to the flavonoid family [13]. These compounds have attracted great interest due to their wide range of pharmacological properties, including mainly anti-inflammatory, analgesic, antipyretic, anti-mutagenic, and anti-leishmanial properties, the anti-proliferative effect they have on cancer cell lines, and their antifungal effects [14–20]. Moreover, chalcones have several applications in agriculture, as insect antifeedant [8], antifungal [9], and larvicidal [10] activities have also been demonstrated for chalcone derivatives. For example, several halogenated chalcones (**1a–f**) have been tested against *B. cinerea* (see Fig. 1), exhibiting growth inhibition activity values between 28 and 67% at the concentration of 100 µg/mL, [11] while natural flavonoids (**2a–i**) tested on the same phytopathogen show weak antifungal activity with growth inhibition activity between 2.0 and 37% [12] at the concentration of 40 µg/mL. However, there is currently no information regarding the effect of chalcones and flavonoids on *M. fructicola*.

A current trend in the discovery and development of highly active compounds is the hybridization of two or more active fragments that may present improved pharmacological activities [21, 22]. Chromanes are small, natural compounds, and fragments of other more complex natural products that are used in this manner. They have attracted intense interest because of their numerous biological activities such as antimicrobial, allergenic, plant growth inhibitory, and anti-herbivore activities and anti-proliferative effects against cancer cell lines [23, 24]. In addition, the saturated derived structure known as dihydrochromane (or tetrahydropyran) is an important structural fragment of the molecules in many biologically active and natural compounds [25, 26], and in particular, antibiotic activity has been identified for this fragment type [27]. As mentioned above, the hybridization of chalcone and dihydrochromane fragments may lead to good *B. cinerea* and *M. fructicola* in vitro inhibition growth mycelial activity (see Fig. 2).

Since the synthesis of organic compounds focused on obtaining a solution for the control of *B. cinerea* and *M. fructicola* postharvest diseases has not been explored in depth, and due to the potential fungicide applications of chalcones, we synthesized ten chalcones (**7a–j**) and five dihydrochromane–chalcones hybrids (**7k–o**) that are reported here for

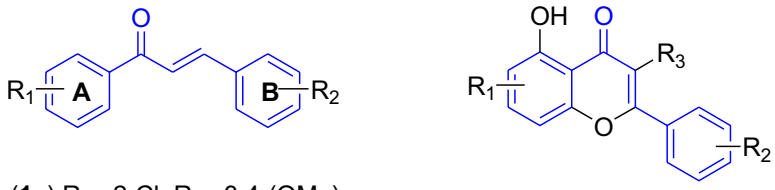

(**1a**) R_1= 2-Cl, R_2= 3,4-$(OMe)_2$
(**1b**) R_1= 3-Cl, R_2= 4-OMe
(**1c**) R_1= 3-Br, R_2= 4-OMe
(**1d**) R_1= 4-F, R_2= 2,4-$(Cl)_2$
(**1e**) R_1=R_2= 2,4-$(Cl)_2$
(**1f**) R_1= 3,4-$(Cl)_2$, R_2= 3,4-$(OMe)_2$

(**2a**) R_1= 3-OMe, 4-OH, R_2= H, R_3= OMe
(**2b**) R_1= 3,4-$(OMe)_2$-5-OH, R_2= H, R_3= OMe
(**2c**) R_1= 4-OMe, R_2= H, R_3= OMe
(**2d**) R_1= 3,4,5-$(OMe)_3$, R_2= H, R_3= OH
(**2e**) R_1= 3,4,5-$(OMe)_3$, R_2= H, R_3= OMe
(**2f**) R_1= 4-OH, R_2= H, R_3= OMe
(**2g**) R_1= 3-OMe-4-OH, R_2= H, R_3= OMe
(**2h**) R_1= 4-OH, R_2=H, R_3= OH
(**2i**) R_1= 4-OH, R_2= 3,4-$(OH)_2$, R_3= OH

Fig. 1 Halogenated chalcones and natural flavonoids with an inhibitory effect on *B. cinerea*

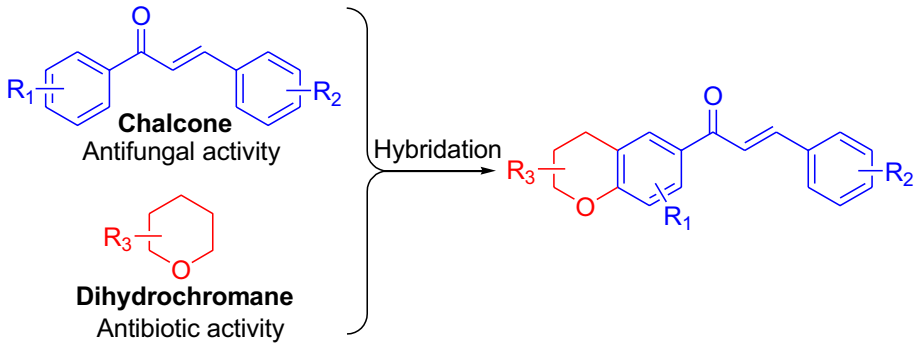

Fig. 2 Chalcone and dihydrochromane structures hybridization for rational design

the first time. In addition, all compounds were evaluated for antifungal activity against *B. cinerea* and *M. fructicola*, and their quantitative structure–activity relationship was studied.

Results and discussion

Chemistry

The compound 1-(4-hydroxy-3-(3-methylbut-2-enyl)phenyl)ethanone (3) was isolated from methanolic extract of *Senecio graveolens* by column chromatography and identified by spectroscopic techniques (IR, NMR, and MS), according to the procedures described in our previous report [28]. Then, compound **3** was converted into 1-(2,2-dimethylchroman-6-yl)ethanone (**4**) by prenyl cycling the group in acidic media [29]. In this reaction, formic acid was used at room temperature, obtaining a crystalline solid with excellent yield (96%, see Scheme 1). The ^{1}H-NMR spectrum shows two triplet signals at $\delta = 2.73$ and $\delta = 1.75$ ppm ($J = 6.7$ Hz), each one with two hydrogen atoms corresponding to the benzylic and homobenzylic CH_2 of the dihydrochromane skeleton. Similarly, the ^{13}C-NMR spectrum shows a quaternary carbon signal at $\delta = 75.5$ ppm corresponding to the carbon bonded to the oxygen of dihydrochromane and two methyl groups. In addition, the spectroscopic data are consistent with the previous report [30]. The final compounds (**7a–o**) were synthesized using semisynthetic acetophenone (**4**) and acetophenones (**5a–b**) with commercial benzaldehydes (**6a–e**) by Claisen–Schmidt condensation in alkaline media, showing acceptable to excellent yields (27–99%, see Scheme 1).

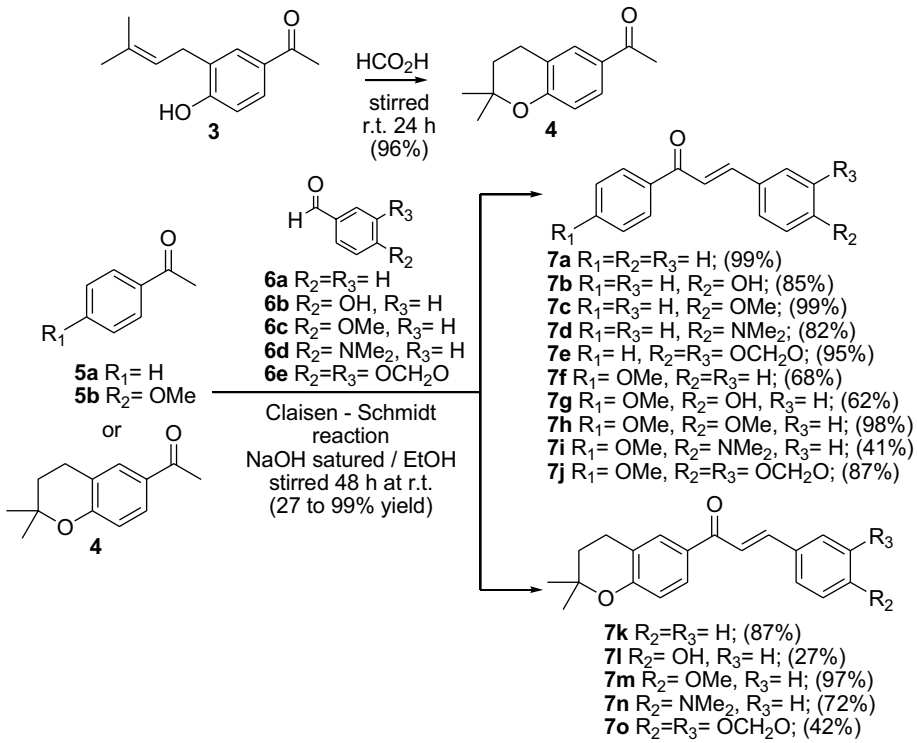

Scheme 1 Synthetic step to obtain compound **4** and final compounds **7a–o**

Table 1 Half-inhibition concentration values (IC_{50}) of compounds **7a–o** on mycelial growth of *B. cinerea* and *M. fructicola*

Compound	*B. cinerea*		*M. fructicola*	
	R^2	$IC_{50} \pm$ S.D.(μg/mL)	R^2	$IC_{50} \pm$ S.D.(μg/mL)
7a	0.992	43.9 ± 1.9[a]	0.946	48.5 ± 1.4[a]
7b	0.919	158.1 ± 1.4	0.922	304.2 ± 1.4
7c	0.938	45.5 ± 1.4[a]	0.91	135.6 ± 1.3
7d	0.992	132.8 ± 1.8	0.893	78.2 ± 1.3[a]
7e	0.968	59.9 ± 1.5	0.985	56.1 ± 1.7[a]
7f	0.984	76.2 ± 1.6	0.971	51.8 ± 1.5[a]
7g	0.968	436.1 ± 1.7	0.952	302.1 ± 1.5
7h	0.863	169.8 ± 1.2	0.828	200.6 ± 1.2
7i	0.985	139.5 ± 1.8	0.969	147.8 ± 1.6
7j	*i*	*i*	0.907	283.2 ± 1.4
7k	0.979	84.0 ± 1.7	0.993	68.7 ± 1.9
7l	0.961	425.9 ± 17.3	0.941	330.2 ± 20.7
7m	0.970	200.7 ± 1.7	0.951	174.1 ± 1.5
7n	0.957	410.4 ± 1.7	0.970	63.2 ± 1.6[a]
7o	0.963	502.8 ± 1.7	0.957	255 ± 1.7
Captan®	0.972	24.7 ± 1.7[a]	–	–
Mystic®	–	–	0.963	21.6 ± 1.7[a]
Negative Control	*i*	*i*	*I*	*i*

i inactive compound at maximum dose

[a]Significant differences ($p > 0.05$) compared with Captan® or Mystic®

The structures of the final compounds (**7a–o**) were determined using spectroscopic evidence (IR, NMR, and MS, see Electronic Supplementary Material spectra S1–S39). Infrared spectra of all compounds show an absorption peak of the typical conjugated carbonyl group ($\upsilon \sim 1660$ cm^{-1}). In the ^{1}H-NMR, two hydrogen atoms coupling as a doublet downfield are observed ($\delta \sim 7.78$ and 7.42 ppm, $J \sim 15.6$ Hz), corresponding to β- and α-hydrogen atoms with *trans* geometry. For known compounds (**7a–j**), spectroscopic information was compared with previous reports [31–35]. In addition, for the compounds (**7k–o**) reported for the first time, the ^{13}C-NMR and bidimensional NMR experiments (2D-HSQC and 2D-HMBC) showed two carbon signals of CH at $\delta \sim 143$ and 117 ppm bonded to Hβ and Hα, respectively. Moreover, using the 2D-HMBC experiment, it was shown that this hydrogen (Hβ and Hα)was correlated with the quaternary carbons ($\delta \sim 130$ and 120 ppm) of both aromatic rings and the carbonyl group, confirming the Ar–CO–CH = CH–Ar system that is typical of the chalcone structure. Finally, the complete structural assignment of new compounds was carried out using 2D-HSQC and 2D-HMBC experiments, and mass spectrometry was used to complement this information.

Antifungal evaluation

All compounds were tested in vitro using the radial growth rate assay, and it was found that they inhibit growth compared with the negative control (carrier solvent) [36, 37]. The inhibition concentrations that caused 50% mycelia inhibition growth of *B. cinerea* and *M. fructicola* for each compound (**7a–o**) were calculated. The results for the tested compounds on *B. cinerea* showed that the activities range between 43.9 and 502.8 μg/mL, while they range between 48.5 and 330.2 μg/mL for *M. fructicola*. The values obtained for both ascomycetes are summarized in Table 1.

For the set of samples tested against *B. cinerea*, **7a** and **7c** compounds have similar activity to that of Captan® ($p > 0.05$, see Table 1 and Electronic Supplementary Material Fig. S1). The most active compounds (**7a** and **7c**) are small and structurally simple chalcones and show better activity values than the more complex molecules such as the pyrazolo[1,5-*a*] pyrimidine derivatives reported by Zhang et al. [38] Similarly, comparing our results with other nitrogen heterocycles such as the azoles, **7a** and **7c** have similar activities to some of the compounds reported by Zhang et al. [39]. In contrast, for *M. fructicola*, compounds **7a**, **7d**, **7e**, **7f**, and **7n** have similar activities to that of the positive control Mystic® ($p > 0.05$); however, there is no information on the effect of chalcone-structure-related compounds on *M. fructicola*.

Comparing the influence of the methoxy group on ring A (compounds **7f–j**) with the hydrogen substituent (**7a–e**) showed that the methoxy group decreases the activity in *B. cinerea* and the same effect is shown in *M. fructicola* (see Table 1). For the new compounds that contain a dihydrochromane fragment (compound **7k–o**), the activity on *B. cinerea* declines for all compounds, while for *M. fructicola* the effects do not change with the presence of this fragment. The results show that structural modifications of the donor electron group (e.g., OMe) or lipophilic fragment (e.g., dihydrochromane) are not the key features of an increase in the inhibition of activity on *B. cinerea* and *M. fructicola*, while an electronegative group (e.g., F, Cl, or Br) could slightly increase this property [11].

Comparing the substituents in ring B and their effect on the mycelial growth inhibition activity on *B. cinerea*, it was found that the most active substituent is hydrogen (**7a**, **7f**, and **7k**), while the 3,4-dioxomethylen fragment decreases mycelial growth inhibition activity (**7f** and **7o**), except in compound **7e**. For *M. fructicola*, the hydrogen substituent increased the mycelial growth inhibition activity (**7a** and **7f**), except in the compound **7n** that has a 4-NMe_2 fragment, while the substituent in ring B that decreases the activity is the 4-OH fragment (**7b**, **7g**, and **7l**). In this sense, several biological activities of chalcones and structurally related compounds have been linked to their substituent on aromatic rings, e.g., the presence of the hydroxyl group affects the

mycelial growth inhibition in *B. cinerea* and may be related to its cell death mechanism on this phytopathogen [40].

On the other hand, compounds **7a**, **7e**, **7f**, and **7k** showed high activity in both phytopathogens ($IC_{50} < 90$ µg/mL, see Table 1). Compounds **7a**, **7f**, and **7k** have a hydrogen substituent on ring B. Moreover, compound **7c** shows selectivity for *B. cinerea* (threefold higher activity than for *M. fructicola*, see Table 1), and a similar trend was shown by **7h**, while both compounds have the 4-OMe substituent in ring B, the dihydrochromane–chalcone with the same substituent (**7m**) has no selectivity for *B. cinerea*.

In addition, only the dihydrochromane–chalcone compound **7n** shows selectivity for *M. fructicola* (more sixfold higher activity than for *B. cinerea*). However, compounds **7d** and **7i** that have the dimethylamino group linked to ring B have no specific action on either of the phytopathogens (see Table 1).

The global analysis of the relationship between the structural features and fungicidal activity of the tested compounds is presented in the following section.

Structure–activity relationship study

Quantitative structure–activity relationship (QSAR) studies seek to correlate biological activity (e.g., pIC_{50}) with different physicochemical descriptors of a series of compounds. For this purpose, multilinear equations are sought between the activity (dependent variable) and various physicochemical descriptors (independent variables), or structural parameters (e.g., Free–Wilson descriptors). Therefore, the importance of QSAR equations is that they allow the interpretation of the biological results obtained based on the physicochemical properties and the structure of the molecules, and, on the other hand, they allow the design and prediction of biological activity of new molecules not yet synthesized.

To elucidate the structure–activity relationship of the compounds evaluated against *B. cinerea* and *M. fructicola*, a total of 70 descriptors were calculated (see "Materials and methods" section). The formulation of the equations was carried out using a complete training set, as reported in other QSAR works done with a limited number of molecules [41]. The calculations were done in the gaseous phase and in the solvent phase. Multivariate correlations between the descriptors and the biological activity expressed as pIC_{50} were sought according to the procedures described in our previous reports [35, 42]. For both phytopathogens, the best models were obtained in the gas phase (see Electronic Supplementary Material). The final equations were selected based on the values of q^2 and r^2, selecting those with the least number of chemical descriptors.

$$\mathbf{pIC_{50}} = 3.899 - 0.050\mathbf{HA}^2 - 0.468\mathbf{HD} - 1.923\mathbf{C}_5^2 \quad (1)$$

$$n = 12,\ r = 0.921,\ r^2 = 0.848,$$
$$\mathrm{SD} = 0.152,\ F = 14.9,\ n1 = 3.446 \times 10^{-1},$$
$$n2 = 2.309 \times 10^{-2},\ q^2 = 0.821$$

Equation (1) corresponds to the QSAR model for *B. cinerea*. It is observed that inhibitory activity depends on the number of hydrogen bond acceptor (HA) and donor (HD) atoms. The use of these descriptors in QSAR studies has

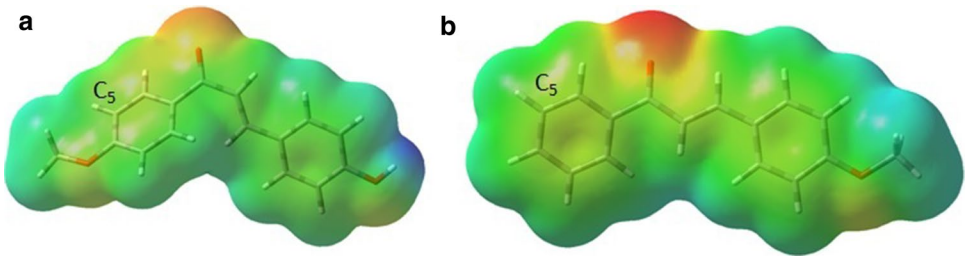

Fig. 3 Electrostatic potential maps of the compounds evaluated in *B. cinerea*. **a** Most active compound **7c. b** Least active compound **7g**

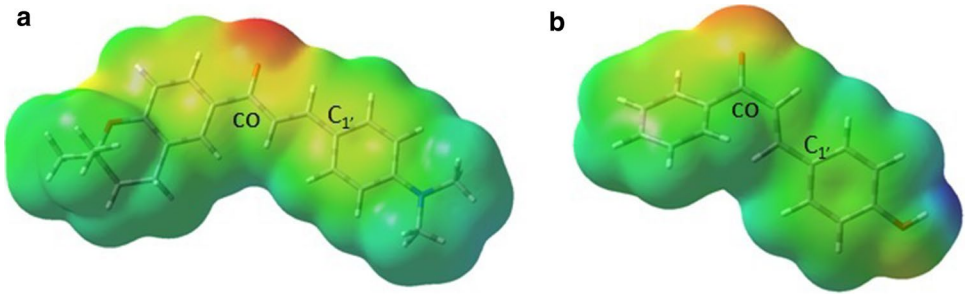

Fig. 4 Electrostatic potential maps of the compounds evaluated for *M. fructicola*. **a** Most active compound **7n. b** Least active compound **7b**

been indicated to be significant due to their importance in the modes of action of the drugs [43, 44]. The activity shows a nonlinear dependence on the number of hydrogen bond acceptor groups. Therefore, the presence of more than one hydrogen bond acceptor group would significantly reduce the activity. On the other hand, the mycelial growth inhibition activity decreases with the square of the electrical charge on the C_5 carbon atom. Using this information and using compound **7c** as the template (Fig. 3a), 22 compounds were proposed and the charge at C_5 was calculated (see Electronic Supplementary Material Table S5). It was found that fluorine or chlorine atoms bonded to C_2, with methyl group bonded to C_5 position, decrease the electron population on C_5 (see Electronic Supplementary Material Table S5, compounds 7 and 8), Therefore, reducing the atomic charge to a value close to zero in C_5 increases the antifungal activity in *B. cinerea*. Additionally, in the simplest compound (**7a**), an appropriate atomic charge distribution was achieved with the 3,4-dibromide, 3-fluorine, 3-bromine-4-chlorine, and 3-methyl substitutions (see Electronic Supplementary Material Table S5, compounds 15, 16, 20, and 22).

Figure 3 shows the electrostatic potential map of compounds **7c** and **7g** that are the most active and least active compounds of this series of compounds, respectively. It is observed that the insertion of a methoxy group in compound **7c** significantly reduces the charge density on the C_5 position (green color in **7c**, see Fig. 3a) compared to that for **7g** (yellow color, see Fig. 3b), which indirectly reduces the red surface on the carbonyl oxygen (see Fig. 3). Therefore, the insertion of electron-donating groups in the *para*-position with respect to the carbonyl group will be favorable for the activity.

Equation (2) describes the QSAR model for *M. fructicola*. It is observed that the inhibitory activity depends on the dipole moment (DM) and the electron density on the $C_{1'}$ carbons and CO. The DM is related to the size and shape of the molecules and to the heterogeneity of the charges on the molecular surface [45, 46]. DM has been previously used in QSAR models to explain the insecticidal activity of *spinosyns* and *spinosoids* [47].

$$\mathbf{pIC}_{50} = 1.600 + 0.014\mathbf{DM}^2 + 9.754\mathbf{C}_{1'}^2 + 3.372\mathbf{CO}^2 \quad (2)$$

$$n = 13,\ r = 0.926,\ r^2 = 0.857,\ \mathrm{SD} = 0.131,$$
$$F = 17.9,\ n1 = 3.068 \times 10^{-1},$$
$$n2 = 1.710 \times 10^{-2},\ q^2 = 0.833$$

The biological activity shows a more significant dependence on the electric charges on the carbonyl carbon. This suggests that the carbonyl group plays an important role in the mechanism of inhibitory action, possibly through hydrogen bonding with the target, and Michael-type reactions [48]. Figure 4 shows the potential electrostatic maps for the most active (**7n**) and least active (**7b**) compounds for *M. fructicola*. Comparison of these two compounds shows that **7n** has a higher electron density on the oxygen atom (red color, Fig. 4a). This is due to the resonance effect of the dihydrochrome system on ring A and the resonance of the dimethylamine group on ring B. This increased polarization of the carbonyl group leads to increased antifungal activity (Eq. 2). On the other hand, the lower negative charge density on the oxygen atom of the carbonyl group in compound **7b** (red color, Fig. 4b) leads to a decrease in the carbon polarization of this functional group (green color, Fig. 4b) and, consequently, the antifungal activity of chalcones for *M. fructicola* is decreased.

Moreover, for $C_{1'}$ atomic charge, compound **7n** is more negative than **7b** (yellow in Fig. 4a and green color in Fig. 4b). Thus, an electron donor substituent on the *ortho*-position of $C_{1'}$ will increase the electron density on $C_{1'}$ and will also increase the antifungal activity of chalcone for *M. fructicola* (see Electronic Supplementary Material Table S6).

Conclusions

In summary, 15 compounds were synthesized and characterized by classical spectroscopic techniques, of which five are reported here for the first time (**7k–o**). In addition, all compounds were tested against *B. cinerea* and *M. fructicola*, obtaining two and five compounds, respectively, with fungicide activity similar to a commercial control (Captan® and Mystic®, respectively). Using the antifungal activity results, quantitative structure–activity relationship models were developed obtaining two models with good statistical parameters (q^2 and r^2 higher than 0.8), identifying the key structural features for the design of new molecules with chalcone as the pharmacophoric core.

Materials and methods

General

Melting point was measured using a Fischer Scientific apparatus (Pittsburgh, PA, USA). Infrared spectra were recorded using the Buck Scientific M500 instrument (Norwalk, CT, USA). The recorded range of the IR spectra was 600 cm^{-1}–4000 cm^{-1}, and all samples were examined using ATR (attenuated total reflectance) system. ^{1}H-NMR, ^{13}C-NMR, 2D-HSQC, and 2D-HMBC spectra were recorded using a Bruker Avance 400 digital NMR spectrometer (Berlin, Germany), operating at 400.13 MHz for ^{1}H and 100.6 MHz for ^{13}C. Chemical shifts are reported in δ (ppm downfield from the TMS resonance), and coupling constants

(*J*) are given in Hz. GC–MS was carried out using an Agilent Technologies 6890 instrument (Santa Clara, CA, USA) with automatic ALS and HP MD 5973 mass detector in the splitless mode. The high-resolution mass spectrometry electronic impact (HR-EI-MS) measurements were taken with a VG Autoespect mass spectrometer (Fision, Ipswich, UK).

Plant material and extraction procedure

Senecio graveolens was collected from an area near Chungara Lake at 4500 m.a.s.l. (Chile). The dry plant material (principally flowers, leaves, and stems, total 180 g) was macerated in 95% ethanol (2 × 500 mL) for 72 h, according to the procedures described in our previous reports [28]. The specimen collection is conserved at CODECITE-CIHDE, Arica, Chile.

Chemistry

(4-Hydroxy-3-(3-methylbut-2-enyl)phenyl)ethanone (3)

This compound was separated from dry methanol extract (52.8 g) by column chromatography using EtOAc/hexane (1:9), obtaining a pale yellow solid (1.09 g, 0.6% yield). MP: 95–96 °C. The spectroscopic information (IR, ^{1}H-NMR, and ^{13}C-NMR) and the MS analysis results were consistent with the previous report [28].

1-(2,2-Dimethylchroman-6-yl)ethanone (4)

In a 250-mL round-bottomed flask, prenyl-acetophenone **3** (1.0 g) and formic acid (30 mL) were added. The mixture was stirred at room temperature for 24 h. Finally, the acid was neutralized using Na_2CO_3 5%. This mixture was extracted with EtOAc (3 × 50 mL), and the organic layer was dried with Na_2SO_4 and separated by column chromatography using an EtOAc–hexane mixture (2:8) obtaining 0.955 g of colorless solid (96% yield). MP: 91–92 °C. IR: υ/cm^{-1} 2991, 2933, 1665, 1613, 1482, 1339, 1327, 1230, 1193; ^{1}H-NMR (400 MHz, $CDCl_3$): δ 7.65 (1H, d, J = 3.4 Hz, H2), 7.62 (1H, dd, J = 8.4, 3.4 Hz, H6), 6.71 (1H, d, J = 8.4 Hz, H5), 2.73 (2H, t, J = 6.7 Hz, CH_2 -C1′), 2.45 (3H, s, CH_3CO), 1.75 (2H, t, J = 6.7 Hz, CH_2-C2′), 1.27 (6H, s, CH_3-C4′ + CH_3-C5′). ^{13}C-NMR (100 MHz, $CDCl_3$): δ 197.0 (C=O), 158.6 (C4), 130.5 (C2), 129.3 (C1), 128.3 (C6), 120.7 (C3), 117.2 (C5), 75.5 (C3′), 32.5 (C2′), 26.9 (CH_3CO + C4′*), 26.3 (C5′*), 22.3 (C1′). * Interchangeable signals. ^{1}H-NMR, ^{13}C-NMR, and MS analyses results are consistent with the previous report [30].

General procedure for chalcone synthesis (7a–o)

To a dry, 100-mL round-bottomed flask, acetophenone **4** or **5a–b** (250 mg, between 1.22 and 2.08 mmol) and commercial benzaldehyde **6a–e** (1.2 molar equivalents) were added. Both reagents were solubilized in ethanol (5 mL), a NaOH-saturated solution was added (in 10 mL of ethanol), and the mixture was stirred for 48 h, after which 5% HCl solution was added until pH ~ 7 to end the reaction, and the mixture was extracted with EtOAc (3 x 30 mL). The organic layer was dried with Na_2CO_3, filtered, and separated with column chromatography using a hexane/EtOAc mixture increased polarity, obtaining compounds **7a–o** in yields between 27 and 99%.

(*2E*)-1,3-diphenylprop-2-en-1-one (7a)

Yellow solid (99% yield). MP: 65–69 °C. IR: υ_{max}/cm^{-1} 3069, 2970, 1682, 1606, 1518, 1420; ^{1}H-NMR (400 MHz, $CDCl_3$): δ 8.03 (2H, d, J = 7.5 Hz, H2′ + H6′), 7.82 (1H, d, J = 15.6 Hz, Hβ), 7.65 (2H, m, H2 + H6), 7.59 (1H, t, J = 7.5, Hz, H4), 7.54 (1H, d, J = 15.6 Hz, Hα), 7.52 (2H, d, J = 7.5 Hz, H3 + H5), 7.42 (3H, m, H3′ + H5′ + H4′); ^{13}C-NMR (100 MHz, $CDCl_3$): δ 190.5 (C = O), 144.8 (Cβ), 138.2 (C1), 134.8 (C1′), 132.7 (C4), 130.5 (C4′), 128.9 + 128.6 + 128.5 + 128.4 (C2 + C3 + C5 + C6 + C2′ + C3′ + C5′ + C6′), 122.1 (Cα). ^{1}H-NMR, ^{13}C-NMR, and MS analyses results are consistent with our previous report [35].

(*2E*)-3-(4-hydroxyphenyl)-1-phenylprop-2-en-1-one (7b)

Orange solid (85% yield). MP: 183–187 °C. IR: υ_{max}/cm^{-1} 3421, 3024, 1647, 1594, 1566, 1513, 1180; ^{1}H-NMR (400 MHz, $CDCl_3$): δ 8.11 (2H, d, J = 8.4 Hz, H2 + H6), 7.75 (1H, d, J = 15.6 Hz, Hβ), 7.71 (2H, d, J = 8.9 Hz, H2′ + C6′), 7.61 (1H, d, J = 7.7 Hz, H4), 7.54 (2H, d, J = 7.7 Hz, H3 + H5), 7.53 (1H, d, J = 15.6 Hz, Hα), 6.92 (2H, d, J = 8.9 Hz, H3′ + H5′); ^{13}C-NMR (100 MHz, $CDCl_3$) δ 189.9 (C=O), 160.8 (C4′), 145.2 (Cβ), 139.4 (C1), 133.3 (C4), 131.5 (C2′ + C6′), 129.4 (C3 + C5), 129.1 (C2 + C6), 127.5 (C1′), 119.6 (Cα), 116.7 (C3′ + C5′). ^{1}H-NMR, ^{13}C-NMR, and MS analyses results are consistent with our previous report [35].

(*2E*)-3-(4-methoxyphenyl)-1-phenylprop-2-en-1-one (7c)

Yellow solid (99% yield). MP: 70–72 °C. IR: υ_{max}/cm^{-1} 3066, 2929, 1662, 1596, 1546, 1511, 1466, 1239, 1214;

^{1}H-NMR (400 MHz, $CDCl_3$): δ 8.01 (2H, d, J = 7.5 Hz, H2 + H6), 7.89 (1H, d, J = 15.6 Hz, Hβ), 7.60 (2H, d, J = 8.7 Hz, H2′ + H6′), 7.57 (1H, t, J = 7.5 Hz, H4), 7.49 (2H, d, J = 7.5 Hz, H3 + H5), 7.42 (1H, d, J = 15.6 Hz, Hα), 6.93 (2H, d, J = 8.7 Hz, H3′ + H5′), 3.85 (3H, s, C$\underline{H}_3$O-C4′); ^{13}C-NMR (100 MHz, $CDCl_3$): δ 190.5 (C=O), 161.6 (C4′), 144.7 (Cβ), 138.4 (C1), 132.5 (C4), 130.2 (C2′ + C6′), 128.5 (C2 + C6), 128.4 (C3 + C5), 127.5 (C1′), 119.7 (Cα), 114.4 (C3′ + C5′), 55.4 ($\underline{C}H_3$O-C4′). ^{1}H-NMR, ^{13}C-NMR, and MS analyses are consistent with our previous report [35].

(2*E*)-3-[4-(dimethylamino)phenyl]-1-phenyl-prop-2-en-1-one (7d)

Orange solid (82% yield). MP: 109–111 °C. IR: υ_{max}/cm^{-1} 3062, 2966, 1644, 1564, 1532, 1486, 1460, 1228, 1167; ^{1}H-NMR (400 MHz, $CDCl_3$): δ 7.99 (2H, d, J = 7.6 Hz, H2 + H6), 7.79 (1H, d, J = 15.5 Hz, Hβ), 7.55 (2H, d, J = 8.6 Hz, H2′ + H6′), 7.54 (1H, m, H4), 7.48 (2H, d, J = 7.5 Hz, H3 + H5), 7.34 (1H, d, J = 15.5 Hz, Hα), 6.73 (2H, d, J = 8.6 Hz, H3′ + H5′), 3.03 (6H, s, $(C\underline{H}_3)_2$N-C4′); ^{13}C-NMR (100 MHz, $CDCl_3$): δ 190.7 (C=O), 145.7 (Cβ), 138.9 (C1), 132.2 (C2′ + C6′), 130.4 (C4), 128.4 (C2 + C6), 128.3 (C3 + C5), 117.2 (Cα), 112.3 (C3′ + C5′), 110.9 (C1′), 40.4 ($(\underline{C}H_3)_2$N-C4′). ^{1}H-NMR, ^{13}C-NMR, and MS analyses results are consistent with our previous report [35].

(2*E*)-3-(1,3-benzodioxol-5-yl)-1-phenyl-prop-2-en-1-one (7e)

Pale yellow solid (95% yield). MP: 48–50 °C. IR: υ_{max}/cm^{-1} 3085, 2958, 2920, 1659, 1607, 1578, 1468, 1225; ^{1}H-NMR (400 MHz, $CDCl_3$): δ 8.00 (2H, d, J = 7.6 Hz, H2 + H6), 7.73 (1H, d, J = 15.6 Hz, Hβ), 7.57 (1H, t, J = 7.6 Hz, H4), 7.48 (2H, d, J = 7.6 Hz, H3 + H5), 7.36 (1H, d, J = 15.6 Hz, Hα), 7.16 (1H, s, H2′), 7.11 (1H, d, J = 8.0 Hz, H6′), 6.83 (1H, d, J = 8.0 Hz, H5′), 6.00 (2H, s, O$C\underline{H}_2$O); ^{13}C-NMR (100 MHz, $CDCl_3$): δ 190.2 (C=O), 149.8 (C4′), 148.3 (C3′), 144.6 (Cβ), 138.3 (C1), 132.5 (C4), 129.2 (C1′), 128.5 (C2 + C6), 128.3 (C3 + C5), 125.1 (C6′), 120.0 (Cα), 108.6 (C2′), 106.6 (C5′), 101.5 (O$\underline{C}H_2$O). ^{1}H-NMR, ^{13}C-NMR, and MS analyses results are consistent with our previous report [35].

(2*E*)-1-(4-methoxyphenyl)-3-phenylprop-2-en-1-one (7f)

Yellow solid (68% yield). MP: 70–72 °C. IR: υ_{max}/cm^{-1} 3078, 2972, 2954, 1655, 1603, 1558, 1508, 1448, 1241, 1190; ^{1}H-NMR (400 MHz, $CDCl_3$): δ 8.01 (2H, d, J = 7.5 Hz, H2 + H6), 7.89 (1H, d, J = 15.6 Hz, Hβ), 7.60 (2H, d, J = 8.7 Hz, H2′ + H6′), 7.57 (1H, t, J = 7.5 Hz, H4′), 7.49 (2H, d, J = 7.5 Hz, H3 + H5), 7.42 (1H, d, J = 15.6 Hz, Hα), 6.93 (2H, d, J = 8.7 Hz, H3′ + H5′), 3.85 (3H, s, C$\underline{H}_3$O-C4′); ^{13}C-NMR (100 MHz, $CDCl_3$): δ 190.5 (C=O), 161.6 (C4′), 144.7 (Cβ), 138.4 (C1), 132.5 (C4), 130.2 (C2′ + C6′), 128.5 (C2 + C6), 128.4 (C3 + C5), 127.5 (C1′), 119.7 (Cα), 114.4 (C3′ + C5′), 55.4 ($\underline{C}H_3$O-C4′). ^{1}H-NMR, ^{13}C-NMR, and MS analyses results are consistent with our previous report [34].

(2*E*)-3-(4-hydroxyphenyl)-1-(4-methoxyphenyl) prop-2-en-1-one (7g)

Yellow solid (62% yield). MP: 184–186 °C. IR: υ_{max}/cm^{-1} 3266, 3086, 2949, 1668, 1605, 1558, 1531, 1229, 1146; ^{1}H-NMR (400 MHz, $CDCl_3$): δ 8.03 (2H, d, J = 8.9 Hz, H2 + H6), 7.77 (1H, d, J = 15.6 Hz, Hβ), 7.56 (2H, d, J = 8.4 Hz, H2′ + H6′), 7.42 (1H, d, J = 15.6 Hz, Hα), 6.98 (2H, d, J = 8.9 Hz, H3 + H5), 6.88 (2H, d, J = 8.4 Hz, H3′ + H5′), 3.89 (3H, s, C$\underline{H}_3$O-C4′). ^{13}C-NMR (100 MHz, $CDCl_3$): δ 188.9 (C=O), 163.3 (C4), 157.7 (C4′), 143.8 (Cβ), 131.3 (C1), 130.7 (C2 + C6), 130.3 (C2′ + C6′), 128.0 (C1′), 119.7 (Cα), 115.9 (C3′ + C5′), 113.8 (C3 + C5), 55.5 ($\underline{C}H_3$O-C4′). ^{1}H-NMR, ^{13}C-NMR, and MS analyses results are consistent with our previous report [34].

(2*E*)-3-(4-methoxyphenyl)-1-(4-methoxyphenyl) prop-2-en-1-one (7h)

Pale yellow solid (98% yield). IR: υ_{max}/cm^{-1} 3062, 2945, 2931, 1654, 1590, 1569, 1509, 1457, 1420, 1246, 1212; ^{1}H-NMR (400 MHz, $CDCl_3$): δ 8.03 (2H, d, J = 8.8 Hz, H2 + H6), 7.77 (1H, d, J = 15.6 Hz, Hβ), 7.59 (2H, d, J = 8.7 Hz, H2′ + H6′), 7.42 (1H, d, J = 15.6 Hz, Hα), 6.96 (2H, d, J = 8.8 Hz, H3 + H5), 6.92 (2H, d, J = 8.7 Hz, H3′ + H5′), 3.87 (3H, s, C$\underline{H}_3$O-C4), 3.83 (3H, s, C$\underline{H}_3$O-C4′); ^{13}C-NMR (100 MHz, $CDCl_3$): δ 188.6 (C=O), 163.2 (C4), 161.4 (C4′), 143.7 (Cβ), 131.2 (C1), 130.6 (C2 + C6), 130.0 (C2′ + C6′), 127.7 (C1′), 119.4 (Cα), 114.3 (C3 + C5), 113.7 (C3′ + C5′), 55.4 ($\underline{C}H_3$O-C4), 55.3 ($\underline{C}H_3$O–C4′). ^{1}H-NMR, ^{13}C-NMR, and MS analyses results are consistent with our previous report [34].

(2*E*)-3-(4-N,N-dimethylaminephenyl)-1-(4-methoxy-phenyl)prop-2-en-1-one (7i)

Orange solid (98% yield). MP: 122–124 °C. IR: υ_{max}/cm^{-1} 3079, 2979, 2933, 1648, 1579, 1546, 1522, 1435, 1252, 1231, 1162; ^{1}H-NMR (400 MHz, $CDCl_3$): δ 8.03 (2H, d, J = 8.9 Hz, H2 + H6), 7.78 (1H, d, J = 15.4 Hz, Hβ), 7.55 (2H, d, J = 8.6 Hz, H2′ + H6′), 7.36 (1H, d, J = 15.4 Hz, Hα), 6.97 (2H, d, J = 8.9 Hz, H3 + H5), 6.69 (2H, d, J = 8.6 Hz, H3′ + H5′), 3.88 (3H, s, C$\underline{H}_3$O-C4), 4.04 (6H, s, $(C\underline{H}_3)_2$N); ^{13}C-NMR (100 MHz, $CDCl_3$): δ 188.9 (C=O), 162.9 (C4), 151.9 (C4′), 144.9 (Cβ), 131.8 (C1), 130.5 (C2 + C4), 130.2 (C2′ + C4′), 122.8 (C1′), 116.4 (Cα), 113.6 (C3 + C5),

111.8 (C3′ + C5′), 55.4 (C$\underline{H}_3$O-C4), 40.1 (N($\underline{C}H_3)_2$-C4′)). ^{1}H-NMR, ^{13}C-NMR, and MS analyses results are consistent with our previous report [34].

(2*E*)-3-(1.3-benzodioxol-5-yl)-1-(4-methoxyphenyl) prop-2-en-1-one (7j)

Yellow solid (41% yield). MP: 127–133 °C. IR: υ_{max}/cm^{-1} 3078, 2950, 2921, 1661, 1598, 1510, 1466, 1425, 1251, 1218; ^{1}H-NMR (400 MHz, $CDCl_3$): δ 8.03 (2H, d, J = 8.9 Hz, H2 + H6), 7.73 (1H, d, J = 15.5 Hz, Hβ), 7.39 (1H, d, J = 15.5 Hz, Hα), 7.17 (1H, d, J = 1.5 Hz, H2′), 7.12 (1H, dd, J = 8.0, 1.5 Hz, H6′), 6.98 (2H, d, J = 8.9 Hz, H3 + H5), 6.89 (1H, d, J = 8.0 Hz, H5′), 6.03 (2H, s, OC$\underline{H}_2$O), 3.89 (s, C$\underline{H}_3$O-C4). ^{13}C-NMR (100 MHz, $CDCl_3$): δ 188.5 (C=O), 163.3 (C4), 149.7 (C4′), 148.3 (C3′), 143.7 (Cβ), 131.2 (C1), 130.6 (C2 + C6), 129.5 (C1′), 124.9 (C6′), 119.8 (Cα), 113.7 (C3 + C5), 108.6 (C2′), 106.6 (C5′), 101.5 (O$\underline{C}H_2$O), 55.4 ($\underline{C}H_3$O-C4). ^{1}H-NMR, ^{13}C-NMR, and MS analyses results are consistent with our previous report [34].

(2*E*)-1-(2,2-dimethylchroman-6-yl)-3-phenyl-prop-2-en-1-one (7k)

Pale yellow solid (87% yield). MP: 85–87 °C. IR: υ/cm^{-1} 3050, 2975, 2938, 1659, 1604, 1574, 1495, 1448, 1336, 1258, 1230; ^{1}H-NMR (400 MHz, $CDCl_3$): δ 7.83 (1H, dd, J = 8.2, 2.6 Hz, H6), 7.82 (1H, d, J = 2.6 Hz, H2), 7.80 (1H, d, J = 15.7 Hz, Hβ), 7.64 (1H, m, H4′), 7.56 (1H, d, J = 15.7 Hz, Hα), 7.40 (4H, m, H2′ + H3′ + H5′ + H6′), 6.86 (1H, d, J = 8.2 Hz, H5), 2.85 (2H, t, J = 6.7 Hz, C$\underline{H}_2$-C1″), 1.85 (2H, t, J = 6.7 Hz, C$\underline{H}_2$-2″), 1.37 (6H, s, C$\underline{H}_3$-C4″ + C$\underline{H}_3$-C5″); ^{13}C-NMR (100 MHz, $CDCl_3$): δ 188.7 (C=O), 158.5 (C4), 143.4 (Cβ), 135.1 (C1′), 130.8 (C5), 130.1 (C2), 128.9 (C2′ + C6′), 128.8 (C4′), 128.4 (C6), 128.3 (C3′ + C5′), 121.9 (C3), 120.9 (C1), 117.3 (Cα), 75.5 (C3″), 32.5 (C2″), 26.9 (C4″ + C5″), 22.3 (C1″). EI-MS (+) *m/z* 292 [M$^+$] (100%). HR-EI-MS (+) 292.1463 calc, 292.1461 found (Δ = 0.0002).

(2*E*)-1-(2,2-dimethylchroman-6-yl)-3-(4-hydroxy-phenyl)prop-2-en-1-one (7l)

Yellow solid (27% yield). MP: 158-160 °C. IR: υ/cm^{-1} 3226, 2971, 2941, 1647, 1602, 1574, 1512, 1446, 1343, 1321, 1231; ^{1}H-NMR (400 MHz, $CDCl_3$): δ 7.83 (1H, d, J = 1.3 Hz, H2), 7.81 (1H, dd, J = 8.5, 1.3 Hz H6), 7.76 (1H, d, J = 15.5 Hz, Hβ), 7.52 (2H, d, J = 8.4 Hz, H2′ + H6′), 7.42 (1H, d, J = 15.5 Hz, Hα), 6.92 (2H, d, J = 8.4 Hz, H3′ + H5′), 6.85 (1H, d, J = 8.5 Hz, H5), 2.84 (2H, t, J = 6.7 Hz, C$\underline{H}_2$-C1″), 1.84 (2H, t, J = 6.7 Hz, C$\underline{H}_2$-C2″), 1.36 (6H, s, C$\underline{H}_3$-C4″ + C$\underline{H}_3$-C5″); ^{13}C-NMR (100 MHz, $CDCl_3$): δ 190.0 (C=O), 158.7 (C4 + C4′), 144.5 (Cβ), 132.5 (C2), 131.0 (C3), 130.4 (C2′ + C6′), 128.6 (C1′), 127.3 (C6), 121.0 (C1), 119.2 (C5), 117.4 (Cα), 116.1 (C3′ + C5′), 75.7 (C3″), 32.5 (C2″), 26.9 (C4″ + C5″), 22.4 (C1″). EI-MS (+) m/z 308 [M +] (100%). HR-EI-MS (+) calc 308.1412, found 308.1417 (Δ = − 0.0005).

(2*E*)-1-(2,2-dimethylchroman-6-yl)-3-(4-methoxy-phenyl)prop-2-en-1-one (7m)

Yellow solid (97% yield). MP: 79–81 °C. IR: υ/cm^{-1} 3082, 2975, 1655, 1589, 1510, 1492, 1338, 1318, 1227; ^{1}H-NMR (400 MHz, $CDCl_3$): δ 7.83 (1H, d, J = 1.2 Hz, H2), 7,81 (1H, dd, J = 8.4, 1.2 Hz, H6), 7.77 (1H, d, J = 15.6 Hz, Hβ), 7.60 (2H, d, J = 8.7 Hz, H2′ + H6′), 7.43 (1H, d, J = 15.6 Hz, Hα), 6.93 (2H, d, J = 8.7 Hz, H3′ + H5′), 6.84 (1H, d, J = 8.4 Hz, H5), 3.85 (3H, s, C$\underline{H}_3$O-C4′), 2.85 (2H, t, J = 6.7 Hz, C$\underline{H}_2$-C1″), 1.85 (2H, t, J = 6.7 Hz, C$\underline{H}_2$-C2″), 1.37 (6H, s, C$\underline{H}_3$-C4″ + CH_3-C5″); ^{13}C-NMR (100 MHz, $CDCl_3$): δ 188.9 (C = O), 161.4 (C4′), 158.4 (C4), 143.4 (Cβ), 130.7 (C2), 130.4 (C3), 130.0 (C2′ + C6′), 128.3 (C1′), 127.9 (C6), 120.9 (C1), 119.7 (C5), 117.2 (Cα), 114.3 (C3′ + C5′), 77.5 (C3″), 55.4 ($\underline{C}H_3$O-C4′), 32.5 (C1″), 26.9 (C2″), 22.3 (C4″ + C5″). EI-MS (+) *m/z* 322 [M$^+$] (100%). HR-EI-MS (+) 322.1569 calc, 322.1560 found (Δ = 0.0009).

(2*E*)-3-(4-(dimethylamino)phenyl)-1-(2,2-dimethyl-chroman-6-yl)prop-2-en-1-one (7n)

Red solid (72% yield). MP: 79-82 °C. IR: υ/cm^{-1} 2977, 2922, 1654, 1592, 1558, 1522, 1434, 1366, 1226, 1163; ^{1}H-NMR (400 MHz, $CDCl_3$): δ 7.83 (1H, dd, J = 8.3, 2.2 Hz, H6), 7.80 (1H, d, J = 2.2 Hz, H2), 7.74 (1H, J = 15.5 Hz, Hβ), 7.54 (2H, d, J = 8.8 Hz, H2′ + H6′), 7.36 (1H, d, J = 15.5 Hz, Hα), 6.83 (1H, d, J = 8.3 Hz, H5), 6.69 (2H, d, J = 8.8 Hz, H3′ + H5′), 3.07 (6H, s, ($C\underline{H}_3)_2$N-C4′), 2.85 (2H, t, J = 6.7 Hz, C$\underline{H}_2$-C1″), 1.84 (2H, t, J = 6.7 Hz, C$\underline{H}_2$-C2″), 1.36 (6H, s, C$\underline{H}_3$-C4″ + C$\underline{H}_3$-C5″);^{13}C-NMR (100 MHz, $CDCl_3$): δ 189.0 (C=O), 158.0 (C4), 151.8 (C4′), 144.5 (Cβ), 130.8 (C1), 130.5 (C6), 130.1 (C2′ + C6′), 128.1 (C2), 122.0 (C1′), 120.8 (C3), 117.1 (Cα), 116.8 (C5), 111.8 (C3′ + C5′), 75.3 (C3″), 40.0 (($\underline{C}H_3)_2$N-C4′), 32.5 (C2″), 26.9 (C4″ + C5″), 22.4 (C1″). EI-MS (+) m/z 335 [M +] (100%). HR-EI-MS (+) calc 335.1885, found 335.1895 (Δ = 0.0010).

(2*E*)-3-(benzo[*d*] [1, 3] dioxol-5-yl)-1-(2,2-dimethyl-chroman-6-yl)prop-2-en-1-one (7o)

Yellow solid (42% yield). MP: 158–159 °C. IR: υ/cm^{-1} 3052, 2967, 2941, 1652, 1604, 1576, 1490, 1446, 1360, 1320, 1233; ^{1}H-NMR (400 MHz, $CDCl_3$): δ 7.82 (1H, d,

$J = 1.9$ Hz, H2), 7.80 (1H, dd, $J = 8.2$, 1.9 Hz, H6), 7.72 (1H, d, $J = 15.6$ Hz, Hβ), 7.39 (1H, d, $J = 15.6$ Hz, Hα), 7.17 (1H, s, H2′), 7.12 (1H, d, $J = 8.0$ Hz, H6′), 6.84 (1H, d, $J = 8.2$ Hz, H5), 6.83 (1H, d, $J = 8.0$ Hz, H5′), 6.02 (2H, s, $OC\underline{H}_2O$), 2,85 (2H, t, $J = 6.7$ Hz, $C\underline{H}_2$-C1″), 1.85 (2H, t, J = 6.7 Hz, $C\underline{H}_2$-C2″), 1.37 (6H, s, $C\underline{H}_3$-C4″ + $C\underline{H}_3$-C5″); ^{13}C-NMR (100 MHz, $CDCl_3$): δ 188.7 (C=O), 158.5 (C4), 149.6 (C4′), 148.3 (C3′), 143.4 (Cβ), 130.7 (C1), 130.2 (C1′), 129.6 (C2), 128.3 (C6), 124.9 (C5′), 120.9 (Cα), 120.0 (C3), 117.3 (C6′), 108.6 (C5), 106.2 (C2′), 101.5 (OCH_2O), 75.5 (C3″), 32.5 (C2″), 26.9 (C4″ + C5″), 22.4 (C1″). EI-MS (+) m/z 336 [M +] (100%). HR-EI-MS (+) calc 336.1362, found 336.1360 ($\Delta = 0.0002$).

In vitro antifungal activity of synthetic compounds against *B. cinerea* and *M. fructicola*

The antifungal activity of the synthesized compounds (**7a–o**) against *B. cinerea* and *M. fructicola* was determined using radial growth rate assay in potato dextrose agar (PDA) growth medium (see Electronic Supplementary Materials Fig S1) [49]. The synthesized compounds were dissolved in an ethanol/water solution and were added to a petri dish containing PDA medium at 50 °C. The final tested concentrations were 12.5, 25, 50, 150, 250, and 500 µg/mL for each compound. A mycelium agar disk (4 mm in diameter) of the pathogen fungi was placed in the center of the PDA plates. PDA medium containing 1% ethanol was considered as the negative control (C−), whereas Captan® and Mystic® 520 SC, commercial fungicides (ANASAC, Bayer), were used as the positive control (C+) at the same concentrations and under the same conditions as the test compounds. *B. cinerea* was incubated for 3 days at 23 °C, whereas *M. fructicola* was incubated for 1 week at the same temperature in the dark. Each treatment was replicated three times, and each assay was repeated twice. The diameter of the fungi in the cultures was measured, and the inhibition percentages of mycelial growth for each compound were calculated and compared with the negative control as described in a previous report [50].

From mycelial inhibition percentage values and the concentration (µg/mL), the IC_{50} value was calculated for each compound using a logarithmic equation fit analysis carried out with Origin 8.0 software.

Statistical analysis

The data were reported as the mean values ± standard deviation (SD). One-way ANOVA and post hoc HSD Tukey tests were used with a confidence level of 0.95. The significant differences between the antifungal activity of each compound with those of Captan® or Mystic® were calculated. These statistical analyses were performed using the Statistical 7.0 software.

Computational details

All compounds (**7a–o**) were optimized using DFT-B3LYP-6-31G (d,p) level of theory calculations, and the optimized structures were verified by frequency calculations (obtaining no imaginary frequencies) in the gas phase and using the IEFPCM (water) model as the solvent phase. The descriptors obtained from quantum mechanical calculations such as the dipolar moment (DM), atomic charge from the electrostatic potential (C_1, C_2, C_3, C_4, C_5, C_6, $C_{1'}$, $C_{2'}$, $C_{3'}$, $C_{4'}$, $C_{5'}$, $C_{6'}$, C_α, C_β, CO), highest occupied molecular orbital (HOMO), and lowest unoccupied molecular orbital (LUMO) were obtained directly from the output file, while the chemical potential (µ), hardness (η), softness (S), and electrophilic global index (ω)values were calculated using the following equations.

$$\mu = \frac{\left(E_{\mathrm{LUMO}} + E_{\mathrm{HOMO}}\right)}{2} \tag{3}$$

$$\eta = \frac{\left(E_{\mathrm{LUMO}} - E_{\mathrm{HOMO}}\right)}{2} \tag{4}$$

$$S = \frac{1}{2\eta} \tag{5}$$

$$\omega = \frac{\mu^2}{2\eta} \tag{6}$$

In addition, steric and topological descriptors such as molecular weight (MW), lipophilicity index (CLogP), molar refractivity (MR), molecular surface (MS), molecular volume (MV), hydrogen bonding acceptor (HA), hydrogen bonding donor (HD), Balaban index (BI), molecular topological index (MTI), rotatable bonds (RT), topological diameter (TD), and Wiener index (WI) were obtained using molecular mechanics (MM) optimization carried out with the ChemDraw software.

Structure–activity relationship study

The structure–activity relationship study was carried out using multiple linear regressions as described in our previous report with small changes [34, 35]. We developed several regression models using pIC_{50} ($-\log_{10}(IC_{50})$) in mol L^{-1} units as the dependent variable and all descriptors mentioned above in the gas phase and in the solvent phase as independent variables (DM, C_1, C_2, C_3, C_4, C_5, C_6, $C_{1'}$,

$C_{2'}$, $C_{3'}$, $C_{4'}$, $C_{5'}$, $C_{6'}$, C_{α}, C_{β}, CO HOMO, LUMO, μ, η, S, ω, MW, CLogP, MR, MS, MV, HA, HD, BI, MTI, RT, TD, and WI) in linear and squared form.

In addition, to avoid random correlations between pIC_{50} and any descriptor, cross-validation was carried out using the Golbraikh method as described by:

$$q^2 = 1 - \frac{\sum \left(y_{obs} - y_{calc}\right)^2}{\sum \left(y_{obs} - y_{ave}\right)^2} \quad (7)$$

where y_{obs} is the experimental pIC_{50}, y_{cal} is the pIC_{50} calculated by the QSAR model, and y_{ave} is the average pIC_{50} of all of the compounds used in the QSAR model. An acceptable value of q^2 is equal to or higher than 0.5.

Electronic Supplementary Material: ^{1}H-NMR and ^{13}C-NMR of natural, synthetic, and semisynthetic compounds (spectra S1–34); high-resolution mass spectra of new dihydrochromane–chalcone compounds (**7k–o**, spectra S35–39); structure–activity models for *B. cinerea* and *M. fructicola* in gas and solvent phases (Tables S1–S4); effect of compound **7a** at different concentrations on in vitro mycelial growth inhibition of *B. cinerea* and *M. fructicola* (Fig S1); Table S5: proposed molecules and their C_5 atomic charges based on QSAR model of *B. cinerea*; Table S6: proposed molecules based on QSAR model of *M. fructicola.*

Acknowledgements The authors thank Vicerectoria de Investigación y Estudios Avanzados of Pontificia Universidad Católica de Valparaíso, and Dr. Carlos Echiburu-Chau for the collection and identification of *S. graveolens*.

Authors' contributions KD was involved in design, evaluation, interpretation and discussion of biological activity, and manuscript redaction; AM wrote and proofread the manuscript; LE and MC were involved in spectroscopic analysis and discussion. JM was involved in 2D-QSAR models discussion; ECW isolated and identified *M. fructicola*; MM synthesized and isolated all compounds, was involved in spectroscopic analysis and discussion and development and analysis of 2D-QSAR models, and wrote and proofread the manuscript.

Funding This research was funded by CONICYT Programa Formación de Capital Humano Avanzado 21130456, Postdoctoral Fondecyt grant 3180408, and Vicerectoria de Investigación y Estudios Avanzados of Pontificia Universidad Católica de Valparaíso VRIEA-PUCV "37.0/2017".

Compliance with ethical standards

Conflicts of interest The authors declare no conflict of interest.

References

1. Hou D, Yan C, Liu H, Ge X, Xu W, Tian P (2010) Berberine as a natural compound inhibits the development of brown rot fungus *Monilinia fructicola*. Crop Prot 29(9):979–984
2. Romanazzi G, Feliziani E (2014) *Botrytis cinerea* (gray mold). In: Bautista-Baños S (ed) Postharvest decay, control strategies. Academic Press, New York, pp 131–146
3. Martini C, Mari M (2014) *Monilinia fructicola*, Monilinialaxa (monilinia rot, brown rot). In: Bautista-Baños S (ed) Postharvest decay, control strategies. Academic Press, New York, pp 233–265
4. Williamson B, Tudzynsk B, Tudzynski P, van Kan JAL (2007) *Botrytis cinerea*: the cause of grey mould disease. Mol Plant Pathol 8(5):561–580. https://doi.org/10.1111/J.1364-3703.2007.00417.X
5. Rosslenbroich HJ, Stuebler D (2000) *Botrytis cinerea* - history of chemical control and novel fungicides for its management. Crop Prot 19(8–10):557–561. https://doi.org/10.1016/S0261-2194(00)00072-7
6. Panebianco A, Castello I, Cirvilleri G, Perrone G, Epifani F, Ferrara M, Polizzi G, Walters D, Vitale A (2015) Detection of *Botrytis cinerea* field isolates with multiple fungicide resistance from table grape in Sicily. Crop Prot 77:65–73
7. Soylu EM, Kurt S, Soylu S (2010) In vitro and in vivo antifungal activities of the essential oils of various plants against tomato grey mould disease agent *Botrytis cinerea*. Int J Food Microbiol 143(3):183–189. https://doi.org/10.1016/j.ijfoodmicro.2010.08.015
8. Kumar R, Sharma P, Shard A, Tewary D, Nadda G, Sinha A (2012) Chalcones as promising pesticidal agents against diamondback moth (Plutellaxylostella): microwave-assisted synthesis and structure–activity relationship. Med Chem Res 21(6):922–931
9. Kocyigit-Kaymakcioglu B, Beyhan N, Tabanca N, Ali A, Wedge DE, Duke SO, Bernier UR, Khan IA (2015) Discovery and structure activity relationships of 2-pyrazolines derived from chalcones from a pest management perspective. Med Chem Res 24(10):3632–3644. https://doi.org/10.1007/s00044-015-1415-8
10. Satyavani S, Kanjilal S, Rao M, Prasad R, Murthy U (2015) Synthesis and mosquito larvicidal activity of furanochalcones and furanoflavonoids analogous to karanjin. Med Chem Res 24(2):842–850
11. Zheng Y, Wang X, Gao S, Ma M, Ren G, Liu H, Chen X (2015) Synthesis and antifungal activity of chalcone derivatives. Nat Prod Res 29(19):1804–1810. https://doi.org/10.1080/14786419.2015.1007973
12. Cotoras M, Garcia C, Lagos C, Folch C, Mendoza L (2001) Antifungal activity on *Botrytis cinerea* of flavonoids and diterpenoids isolated from the surface of Pseudognaphalium spp. Bol Soc Chil Quim 46(4):433–440
13. Agrawal A (2011) Pharmacological activities of flavonoids: a review. Int J Pharm Sci Nanotech 4(2):1394–1398
14. Yadav VR, Prasad S, Sung B, Aggarwal BB (2011) The role of chalcones in suppression of NF-kappaB-mediated inflammation and cancer. Int Immunopharmacol 11(3):295–309. https://doi.org/10.1016/j.intimp.2010.12.006
15. Pilatova M, Varinska L, Perjesi P, Sarissky M, Mirossay L, Solar P, Ostro A, Mojzis J (2010) In vitro antiproliferative and antiangiogenic effects of synthetic chalcone analogues. Toxicol Int 24(5):1347–1355. https://doi.org/10.1016/j.tiv.2010.04.013
16. Luo Y, Song R, Li Y, Zhang S, Liu ZJ, Fu J, Zhu HL (2012) Design, synthesis, and biological evaluation of chalcone oxime derivatives as potential immunosuppressive agents. Bioorg Med Chem Lett 22(9):3039–3043. https://doi.org/10.1016/j.bmcl.2012.03.080
17. Kamal A, Prabhakar S, Ramaiah MJ, Reddy PV, Reddy CR, Mallareddy A, Shankaraiah N, Reddy TLN, Pushpavalli SNCVL, Pal-Bhadra M (2011) Synthesis and anticancer activity of chalcone-pyrrolobenzodiazepine conjugates linked via 1,2,3-triazole ring side-armed with alkane spacers. Eur J Med Chem 46(9):3820–3831. https://doi.org/10.1016/j.ejmech.2011.05.050

18. Kocyigit UM, Budak Y, Eliguzel F, Taslimi P, Kilic D, Gulcin I, Ceylan M (2017) Synthesis and carbonic anhydrase inhibition of tetrabromo chalcone derivatives. Arch Pharm 350(12) e1700198
19. Kocyigit UM, Budak Y, Gurdere MB, Erturk F, Yencilek B, Taslimi P, Gulcin I, Ceylan M (2018) Synthesis of chalcone-imide derivatives and investigation of their anticancer and antimicrobial activities, carbonic anhydrase and acetylcholinesterase enzymes inhibition profiles. Arch Physiol Biochem 124(1):61–68. https://doi.org/10.1080/13813455.2017.1360914
20. Burmaoglu S, Yilmaz AO, Polat MF, Kaya R, Gulcin I, Algul O (2019) Synthesis and biological evaluation of novel tris-chalcones as potent carbonic anhydrase, acetylcholinesterase, butyrylcholinesterase and alpha-glycosidase inhibitors. Bioorg Chem 85:191–197. https://doi.org/10.1016/j.bioorg.2018.12.035
21. Otero E, Vergara S, Robledo SM, Cardona W, Carda M, Velez ID, Rojas C, Otalvaro F (2014) Synthesis, leishmanicidal and cytotoxic activity of triclosan-chalcone, triclosan-chromone and triclosan-coumarin hybrids. Molecules 19(9):13251–13266. https://doi.org/10.3390/molecules190913251
22. Singh G, Arora A, Mangat SS, Rani S, Kaur H, Goyal K, Sehgal R, Maurya IK, Tewari R, Choquesillo-Lazarte D, Sahoo S, Kaur N (2016) Design, synthesis and biological evaluation of chalconyl blended triazole allied organosilatranes as giardicidal and trichomonacidal agents. Eur J Med Chem 108:287–300. https://doi.org/10.1016/j.ejmech.2015.11.029
23. Romano E, Raschi AB, Gonzalez AM, Jaime G, Fortuna MA, Hernandez LR, Bach H, Benavente AM (2011) Phytotoxic activities of (2R)-6-hydroxytremetone. Plant Physiol Bioch 49(6):671–675. https://doi.org/10.1016/j.plaphy.2011.02.014
24. Jeffrey CS, Leonard MD, Glassmire AE, Dodson CD, Richards LA, Kato MJ, Dyer LA (2014) Antiherbivore prenylated benzoic acid derivatives from piper kelleyi. J Nat Prod 77(1):148–153. https://doi.org/10.1021/np400886s
25. Sanz MA, Voigt T, Waldmann H (2006) Enantioselective catalysis on the solid phase: synthesis of natural product-derived tetrahydropyrans employing the enantioselective oxa-Diels–Alder reaction. Adv Synth Catal 348(12–13):1511–1515. https://doi.org/10.1002/adsc.200606026
26. Ghosh AK, Anderson DD (2011) Tetrahydrofuran, tetrahydropyran, triazoles and related heterocyclic derivatives as HIV protease inhibitors. Future Med Chem 3(9):1181–1197. https://doi.org/10.4155/Fmc.11.68
27. Thompson CF, Jamison TF, Jacobsen EN (2001) FR901464: total synthesis, proof of structure, and evaluation of synthetic analogues. J Am Chem Soc 123(41):9974–9983
28. Santander J, Otto C, Lowry D, Cuellar M, Mellado M, Salas C, Rothhammer F (2015) Specific gram-positive antibacterial activity of 4-hydroxy-3-(3-methyl-2-butenyl) Acetophenone Isolated from Senecio graveolens. Br Microbiol Res J 5(2):94–106
29. Narender T, Reddy KP, Kumar B (2008) BF(3)center dot OEt(2) mediated regioselective deacetylation of polyacetoxyacetophenones and its application in the synthesis of natural products. Tetrahedron Lett 49(28):4409–4415. https://doi.org/10.1016/j.tetlet.2008.05.020
30. Lizarraga E, Gil DM, Echeverria GA, Piro OE, Catalan CAN, Ben Altabef A (2014) Synthesis, crystal structure, conformational and vibrational properties of 6-acetyl-2,2-dimethyl-chromane. Spectrochim Acta A 127:74–84. https://doi.org/10.1016/j.saa.2014.02.035
31. Batovska D, Parushev S, Slavova A, Bankova V, Tsvetkova I, Ninova M, Najdenski H (2007) Study on the substituents' effects of a series of synthetic chalcones against the yeast Candida albicans. Eur J Med Chem 42(1):87–92. https://doi.org/10.1016/j.ejmech.2006.08.012
32. Ritter M, Martins RM, Rosa SA, Malavolta JL, Lund RG, Flores AFC, Pereira CMP (2015) Green synthesis of chalcones and microbiological evaluation. J Brazil Chem Soc 26(6):1201–1210. https://doi.org/10.5935/0103-5053.20150084
33. Zhang LL, Wang AQ, Wang WT, Huang YQ, Liu XY, Miao S, Liu JY, Zhang T (2015) Co–N–C catalyst for C–C coupling reactions: on the catalytic performance and active sites. Acs Catal 5(11):6563–6572. https://doi.org/10.1021/acscatal.5b01223
34. Mellado M, Madrid A, Martinez U, Mella J, Salas CO, Cuellar M (2018) Hansch's analysis application to chalcone synthesis by Claisen-Schmidt reaction based in DFT methodology. Chem Pap 72(3):703–709. https://doi.org/10.1007/s11696-017-0316-3
35. Mellado M, Madrid A, Reyna M, Weinstein-Oppenheimer C, Mella J, Salas CO, Sanchez E, Cuellar M (2018) Synthesis of chalcones with antiproliferative activity on the SH-SY5Y neuroblastoma cell line: quantitative structure-activity relationship models. Med Chem Res 27(11–12):2414–2425. https://doi.org/10.1007/s00044-018-2245-2
36. Gulcin I, Tel AZ, Kirecci E (2008) Antioxidant, antimicrobial, antifungal, and antiradical activities of Cyclotrichium niveum (Boiss.) Manden and Scheng. Int J Food Prop 11(2):450–471. https://doi.org/10.1080/10942910701567364
37. Gulcin I, Kirecci E, Akkemik E, Topal F, Hisar O (2010) Antioxidant and antimicrobial activities of an aquatic plant: duckweed (Lemna minor L.). Turk J Biol 34:175–188. https://doi.org/10.3906/biy-0806-7
38. Zhang J, Peng JF, Bai YB, Wang P, Wang T, Gao JM, Zhang ZT (2016) Synthesis of pyrazolo[1,5-a]pyrimidine derivatives and their antifungal activities against phytopathogenic fungi in vitro. Mol Divers 20(4):887–896. https://doi.org/10.1007/s11030-016-9690-y
39. Zhang J, Peng JF, Wang T, Kang Y, Jing SS, Zhang ZT (2017) Synthesis and biological evaluation of arylpyrazoles as fungicides against phytopathogenic fungi. Mol Divers 21(2):317–323. https://doi.org/10.1007/s11030-017-9727-x
40. Cotoras M, Mendoza L, Munoz A, Yanez K, Castro P, Aguirre M (2011) Fungitoxicity against *Botrytis cinerea* of a Flavonoid Isolated from *Pseudognaphalium robustum*. Molecules 16(5):3885–3895. https://doi.org/10.3390/molecules16053885
41. Verma RP, Hansch C (2005) An approach toward the problem of outliers in QSAR. Bioorgan Med Chem 13(15):4597–4621. https://doi.org/10.1016/j.bme.2005.05.002
42. Mellado M, Madrid A, Martínez U, Mella J, Salas C, Cuellar M (2017) Hansch's analysis application to chalcone synthesis by Claisen–Schmidt reaction based in DFT methodology. Chem Pap 10:15–20. https://doi.org/10.1007/s11696-017-0316-3
43. Fujita T, Nishioka T, Nakajima M (1977) Hydrogen-bonding parameter and its significance in quantitative structure-activity studies. J Med Chem 20(8):1071–1081. https://doi.org/10.1021/Jm00218a017
44. Raevsky OA, Skvortsov VS (2005) Quantifying hydrogen bonding in QSAR and molecular modeling. SAR QSAR Environ Res 16(3):287–300. https://doi.org/10.1080/10659360500036893
45. Chan K, Jensen NS, Silber PM, O'Brien PJ (2007) Structure-activity relationships for halobenzene induced cytotoxicity in rat and human hepatocytes. Chem Biol Interact 165(3):165–174. https://doi.org/10.1016/j.cbi.2006.12.004
46. Stouch TR, Gudmundsson A (2002) Progress in understanding the structure-activity relationships of P-glycoprotein. Adv Drug Deliver Rev 54(3):315–328
47. Sparks TC, Crouse GD, Durst G (2001) Natural products as insecticides: the biology, biochemistry, and quantitative structure-activity relationships of spinosyns and spinosoids. Pest Manag Sci 57(10):896–905. https://doi.org/10.1002/Ps.358
48. Maydt D, De Spirt S, Muschelknautz C, Stahl W, Muller TJ (2013) Chemical reactivity and biological activity of chalcones and other

alpha, beta-unsaturated carbonyl compounds. Xenobiotica; the fate of foreign compounds in biological systems 43(8):711–718. https://doi.org/10.3109/00498254.2012.754112

49. Soto M, Espinoza L, Chavez MI, Diaz K, Olea AF, Taborga L (2016) Synthesis of new hydrated geranylphenols and in vitro antifungal activity against *Botrytis cinerea*. Int J Mol Sci 17(6):840. https://doi.org/10.3390/ijms17060840
50. Hou Z, Yang R, Zhang C, Zhu LF, Miao F, Yang XJ, Zhou L (2013) 2-(substituted phenyl)-3,4-dihydroisoquinolin-2-iums as novel antifungal lead compounds: biological evaluation and structure-activity relationships. Molecules 18(9):10413–10424. https://doi.org/10.3390/molecules180910413

Affiliations

Marco Mellado[1] · Luis Espinoza[2] · Alejandro Madrid[3] · Jaime Mella[4] · Eduardo Chávez-Weisser[5] · Katy Diaz[2] · Mauricio Cuellar[6]

✉ Marco Mellado
marco.mellado@pucv.cl

✉ Katy Diaz
katy.diaz@usm.cl

[1] Facultad de Ciencias, Instituto de Química, Pontificia Universidad Católica de Valparaíso, Av. Universidad #330, Curauma, Valparaiso, Chile

[2] Departamento de Química, Universidad Técnico Federico Santa María, Av. España 1680, Valparaiso, Chile

[3] Departamento de Química, Facultad de Ciencias Naturales y Exactas, Universidad de Playa Ancha, Avda. Leopoldo Carvallo 270, Valparaiso, Chile

[4] Facultad de Ciencias, Instituto de Química, Universidad de Valparaíso, Av. Gran Bretaña 1111, Valparaiso, Chile

[5] Departamento Laboratorios y Estaciones Cuarentenarias, Servicio Agrícola y Ganadero, Ruta 68 #19100 (Km. 12), Pudahuel, Santiago, Chile

[6] Facultad de Farmacia, Centro de Investigación Farmacopea Chilena, Universidad de Valparaíso, Av. Gran Bretaña 1093, Valparaiso, Chile